Environ Earth Sci (2010) 61:311–322
DOI 10.1007/s12665-009-0344-6

ORIGINAL ARTICLE

Surface electrical resistivity tomography and hydrogeological characterization to constrain groundwater flow modeling in an agricultural field site near Ferrara (Italy)

Micòl Mastrocicco · Giulio Vignoli · Nicolò Colombani · Nasser Abu Zeid

Received: 17 October 2008 / Accepted: 17 September 2009 / Published online: 7 November 2009

Abstract A portion of an unconfined alluvial aquifer located in the Padana Plain (Italy) was characterized following an integrated hydro-geophysical approach. Initially an electrical resistivity tomography (ERT) survey was employed to localize the boundaries of a modest paleochannel body and to design the installation of a groundwater monitoring network. Multilevel slug-tests were performed to estimate the aquifer's saturated hydraulic conductivities. Determined permeability values together with electrical resistivity data were correlated. The correlation resulted in a site specific bi-logarithmic linear relationship. Based on this relationship, punctually determined hydraulic conductivities were spatially extended over the studied flow domain. Finally, continuously measured piezometric heads were used to calibrate a 3D flow model. Sensitivity analysis was performed to confirm the reliability of the reconstructed permeability field, as well as, to assess the minimum number of direct measurements needed to safely characterize the selected aquifer portion. The integration of the ERT survey results with the classical hydrogeological tests can be conveniently applied to constrain the permeability field during flow model calibration. Although the applicability of the determined relationship is site specific, the followed procedure is useful especially when there is a need to optimize the available resources and in case of small-scale pilot studies.

Keywords Electrical resistivity tomography (ERT) · Geophysical methods · Hydraulic properties · Hydraulic testing · Groundwater flow numerical modeling · Unconsolidated sediments

M. Mastrocicco · N. Colombani (✉) · N. A. Zeid
Dipartimento di Scienze della Terra,
Università degli Studi di Ferrara, Ferrara, Italy
e-mail: clo@unife.it

G. Vignoli
Dipartimento di Scienze della Terra,
Università di Padova, Padova, Italy

G. Vignoli
Math4Tech Center, Università degli Studi di
Ferrara, Ferrara, Italy

N. Colombani
Dipartimento di Scienze della Terra,
Università di Roma "La Sapienza", Rome, Italy

Introduction

Hydraulic conductivity distribution is a key parameter for groundwater flow modeling and prediction in projects focusing on aquifer characterization, protection, management and restoration. Unfortunately, an adequate reconstruction of permeability fields based on direct observations is complex, especially in highly heterogeneous alluvial aquifers. On the one hand, borehole data (flow monitoring, geophysical and lithologic logs and cores) are costly, time-consuming and only provide punctual information in the vicinity of the borehole or between closely spaced boreholes. On the other hand, small-scale measurements of hydraulic conductivity are more feasible, for instance, laboratory measurements as Darcy tests and grain size distribution or field measurements as in-well flowmeter and slug tests, with the latter generally recognized as more reliable (Cardenas and Zlotnik 2003). However, such small-scale measurements may be too noisy to be directly used for site-scale flow model calibration (e.g., Barlebo et al. 2004). Therefore, indirect estimates of the hydraulic parameters from surface geophysical surveys,

could provide significant complementary information that may help to reduce the expenses of hydrogeological site investigation (Slater 2007).

The use of direct current (DC) resistivity methods in site investigation alone may be reasonable especially when a prior lithologic information is available; however, in many cases, a unique relationship between resistivity and hydraulic conductivity cannot be found (e.g., Mazac et al. 1985; Purvance and Andricevic 2000). The non-uniqueness is due to the dependency of the hydraulic parameters on both porosity and geometry of the pore spaces, which cannot be uniquely determined using the DC resistivity alone without further assumptions (Slater 2007). Close liaison between electrical resistivity and hydraulic parameters, such as permeability, has been found in many studies (e.g., Kelly 1977; Heigold et al. 1979; Kosinski and Kelly 1981; Urish 1981; Ponzini et al. 1983; Hubbard and Rubin 2000). Sometimes, a simple log–log linear relationship can be established between electrical (σ) and hydraulic conductivities (k) (Purvance and Andricevic 2000). If this is the case, resistivity data can be used as a low cost tool to help mapping the hydraulic conductivity distribution; which, can help to constrain the model calibration (Dam and Christensen 2003).

Many studies have focused on the existing liaison between geophysical determined physical properties and field-scale hydrogeologic properties (Ahamed et al. 1987; Cassiani and Medina 1997; Linde et al. 2006; Bowling et al. 2006). In this way, the increasing complexity of the 3D flow and transport models which requires the 3D distributions of the permeability field, available only at certain well-characterized sites, can be in part resolved (e.g., Bowling et al. 2005; Hess et al. 1992; Rehfeldt et al. 1992). As many sites of hydrogeological interest do not have such details, in this paper it is presented a methodological procedure to locate major sedimentary bodies (such as paleochannels) and to characterize their hydraulic conductivity field employing both electrical resistivity tomography (ERT) technique and hydrogeological field measurements. The procedure was applied in the L.A.R.A. (network laboratory for waters) test Site, located near to Ferrara (NE Italy). Because the unconfined aquifer is vulnerable to fertilizers and pesticides (Dinelli et al. 2000; Mastrocicco et al. 2008), intensively used in the area, it was selected to be characterized with the proposed approach.

The main aim of the present work was to evaluate and quantify possible improvement in the estimation of the hydraulic conductivity distribution, using geophysically derived data obtained from surface resistivity surveys, rather than employing an average permeability or sparse interpolated values.

To gain this goal nine groundwater flow scenarios, using different permeability fields either directly and/or indirectly determined, were used to asses the correspondence between simulated and observed heads. The comparison between results of the nine scenarios allowed to define the minimum hydro-geophysical data set needed to sufficiently characterize the site permeability field.

Materials and methods

Site description

The test site belongs to a rural area of the F.lli Navarra Foundation for Agriculture, located between Ferrara and the Po River, NE Italy, 44°51′32N, 11°39′15E. The Po River valley is the largest Italian alluvial plain, it was formed in the last 30,000 years (Amorosi et al. 2003) as a result of eustatic sea level changes following the latest glacial period. The study area shows few peculiar morphologic highs, reflecting the geomorphologic limits of principal paleo-channel structures. These highs, however, are not useful to single out paleo-river channels of minor entity. The site stratigraphy has been investigated with few core logs (Fig. 1), hence, an appropriate reconstruction of the hydrostratigraphic geometry was not possible. The available subsurface data allowed for the general definition of the hydrogeological units present in the test site: from 0 to approximately 5 m b.g.l., the unconfined aquifer is composed of recent fluvial sandy deposits with clay and silt lenses; from 5 to almost 18 m b.g.l., the aquiclude, is made up of more impermeable clay and silt sediments rich in organic matter and peat. These sediments have been deposited in marsh and lagoon environments, during a period of water stagnation following a rapid sea level rise at the beginning of the present interglacial period (Amorosi et al. 1999, 2003); below 18 m b.g.l, a succession of about 25–30 m thick of sand with few clay and silt lenses of Würmian fluvial deposits hosts the first confined aquifer (Fig. 1).

The two aquifers have different flow directions: the hydraulic gradient of the unconfined aquifer is mainly affected by canals' water level variation; while, the drainage of the deep aquifer is mainly eastward, governed by the regional flux toward the sea (Fig. 1). The groundwater in the area has moderate TDS (total dissolved solids) and nearly constant electrical conductivity ranging between 1 and 1.2 mS/cm.

Electrical resistivity tomography data collection

The ERT survey was carried out in order to select the more suitable area to allocate the field-scale hydrogeological test site. The apparent resistivity data were collected using the ABEM SAS4000/ES464 multi-electrode georesistivity

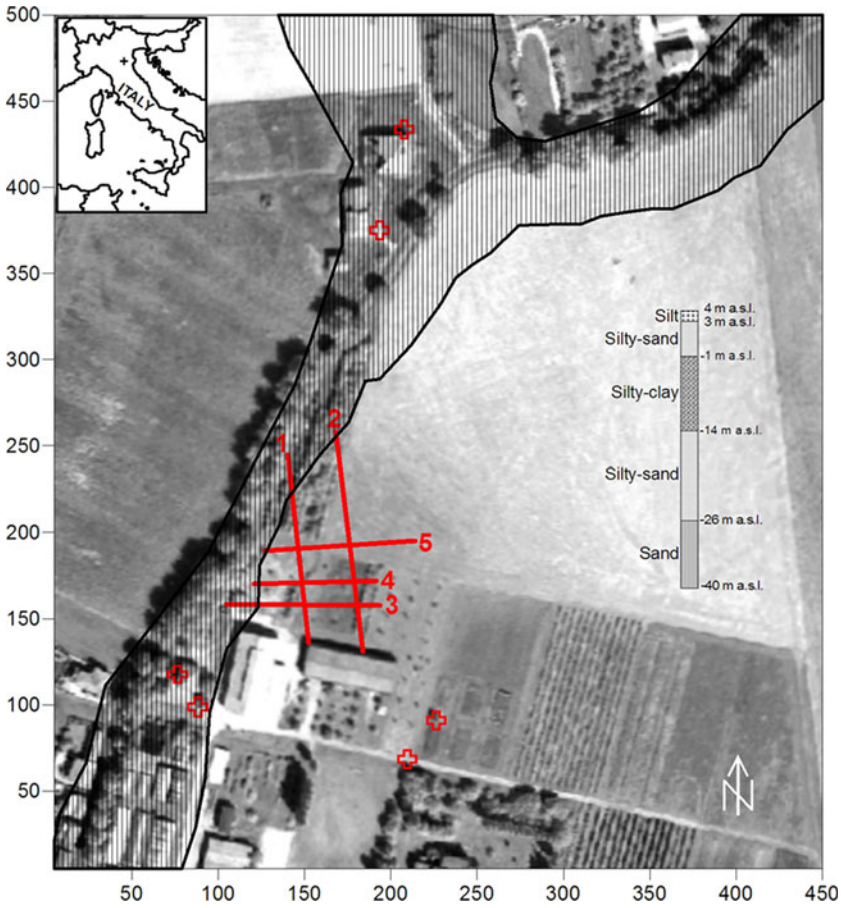

Fig. 1 Quick-Bird satellite image of the test site 1:5,000 (axis ticks are in meters): the cross on the Country map indicates the site location, *shaded area* is a morphological high, *red bold lines* represent the ERT survey lines and *red crosses* are available boreholes with stratigraphy; a typical stratigraphic log is shown in the *inset*

meter. Apparent resistivity data were collected employing the Wenner–Schlumberger and Dipole–Dipole arrays along five profiles (Fig. 1). Electrode spacing ranged between 2.5 and 3 m. Generally data quality was good as the standard deviation of the measured voltages was almost always less than ±1% (two staking cycles with four readings each). Current was always fixed by the georesistivity meter through all the data acquisition phase.

Apparent resistivity data were inverted using the package RES2DINV (Loke 2001), in order to obtain the best estimate of the 2D true resistivity distribution beneath each profile. We performed 2D inversions because collected data are 3D just at first glance; even if survey lines crossing each other, they are too distant to provide 3D information: in order to be considered three-dimensional, profiles should be far closer than nine meters (i.e. three times the inline maximum electrode unit spacing) as it was empirically observed by Dahlin and Loke (1997) and as it can be deduced by studying the three-dimensional sensitivity patterns of Dipole–Dipole and Wenner–Schlumberger arrays. Moreover, our strategy also in the ERT survey planning, kept in mind that one of the main objectives of this work was to minimize the number of data needed to get an acceptable flow model.

Piezometers construction and hydraulic testing

Following the quantitative interpretation of the ERT data, a small area crossing a paleo-channel was selected for further subsurface hydrogeological characterization. For this purpose, 13 continuous core logs were accomplished and equipped with piezometers (Fig. 2). All wells (5–10 cm inner diameter) were screened from 1 m b.g.l. (ground elevation is 4.3 m a.s.l.) to 8 m b.g.l. fully penetrating the unconfined aquifer. The piezometers were sealed with a mixture of cement and bentonite at the top to prevent surface-water infiltration. A detailed topographic survey with a total station Nikon DTM-450, was carried out to accurately determine well case altitudes. Water level changes were recorded with LTC M10 Levelogger Solinst.

Slug tests were used to estimate the hydraulic conductivity in the vicinity of the borehole, although they may be biased by multiple factors (Zlotnik 1994; Hyder and Butler 1995; Butler et al. 1996). The greatest potential bias is a zone of altered hydraulic conductivity immediately surrounding the wellbore caused by drilling disturbance. To minimize this problem, piezometers were modestly developed to virtually eliminate all skin effects during slug testing (Rovey and Niemann 2001).

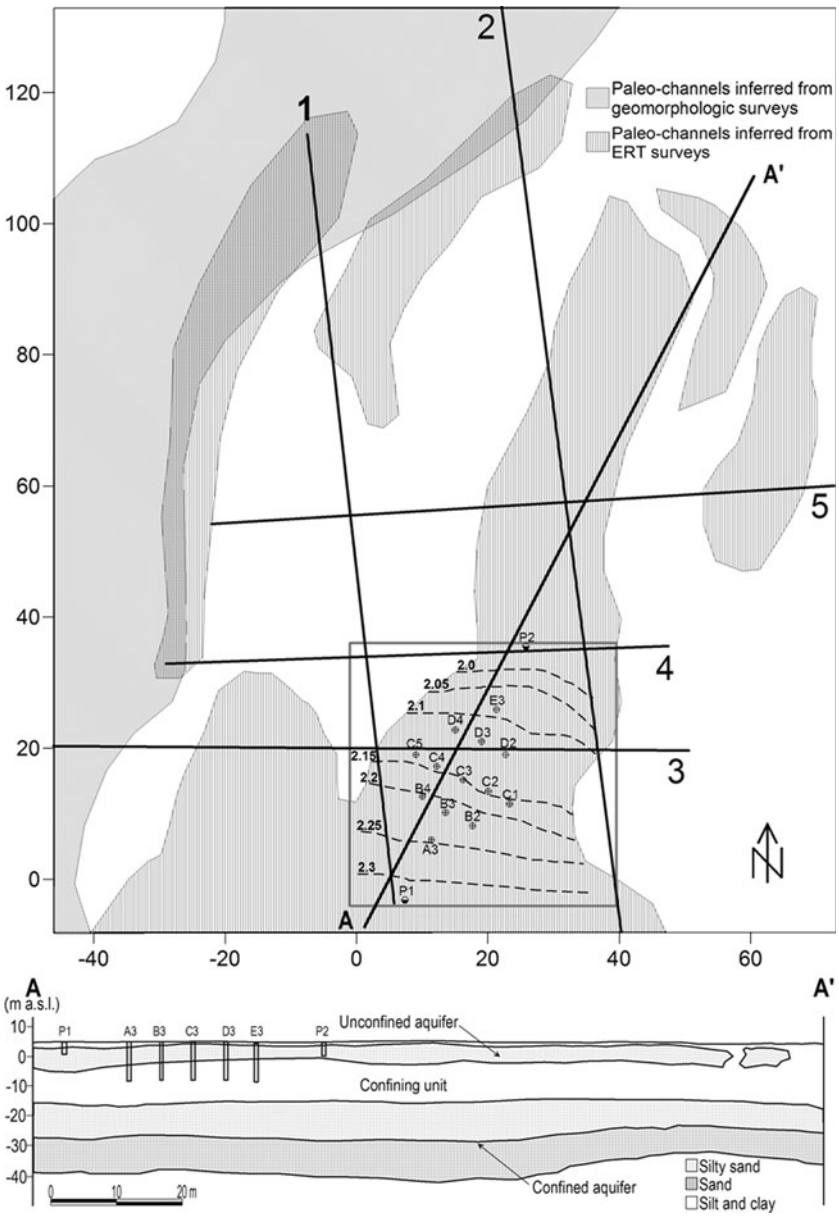

Fig. 2 Paleo-channel reconstruction from geomorphologic and ERT surveys: *dashed lines* are piezometric contours in m a.s.l., *gray box* is the model domain, *bold black lines* represent ERT surveys, 13 cross-circles are new drilled piezometers and two *black-white circles* are auger piezometers

Slug tests were performed in all piezometers at discrete intervals using a straddle-packer assemblage designed to isolate an interval of the aquifer with a length of approximately 0.5 m, a pneumatic initiation system was used to instantaneously lower the static groundwater level of approximately 0.3 m. As water table laid approximately 2 m b.g.l., three slug tests per piezometer were conducted successively over the whole saturated thickness of the unconfined aquifer. Wells were purged before each set of tests. All the acquired slug test responses were overdamped and were analyzed using the Bouwer and Rice (1976) method included in AQTESOLV software (Duffield 2002). Once concluded the hydraulic conductivity characterization, three piezometric surveys were completed, to reconstruct local water table contours at different water level (Fig. 2). At last, piezometers Nos. A3, C1, C5 and E3 were equipped with LTC M10 Levelogger Solinst, to continuously monitor the electrical conductivity, water level and temperature.

Finally, two additional piezometers (2.5 cm inner diameter) were drilled manually with an Ejielkamp Agrisearch auger equipment down to 3 m b.g.l. to monitor groundwater levels (Fig. 2). For each borehole, two 2.5 cm i.d. and 30 cm long undisturbed core samples were recovered using a plexiglass column bevelled at its base, at 1 and 2 m a.s.l., respectively. Cores were cut in two 0.15 m segments for grain size distribution analysis and permeability tests.

Samples for grain size analysis were mixed with H_2O_2 at 16 volumes and allowed to react for 2 days to eliminate the

Table 1 Input parameters used in the flow model

Parameter	Values
Hydraulic conductivity (k)	From $2e^{-7}$ to $2e^{-4}$ m/s
Average hydraulic gradient	3‰
Specific storage (S_s)	0.0001 m^{-1}
Specific yield (S_y)	0.3

organic matter and to avoid the formation of colloids. Afterwards, the fine fraction was separated from the coarse fraction by polypropylene filter with a 63 μm mesh. The coarse fraction was desiccated in oven at 105°C and subdivided mechanically to achieve a sample weighting between 2.8 and 3.2 g. Particle size curves were gained using a sedimentation balance for the coarse fraction and an X-ray diffraction sedigraph model 5100 Micromeritics for the finer fraction; the two regions of the particle size curve were then connected. Hydraulic conductivity values of the four samples were derived according to the widely used Hazen equation (Hazen 1911). A laboratory constant head test was used to determine the saturated hydraulic conductivity of the collected samples (Table 4) and to estimate the specific yield (S_y) and specific storage (S_s) values (Table 1), a single value was used for each parameter since similar results were gained from laboratory tests suggesting a low spatial variation of these parameters.

Groundwater model set-up

Integrating all existing site-specific hydrogeological information, a three-dimensional, transient groundwater flow model was developed to understand the general flow pattern and its variability at the site. Visual MODFLOW 4.2 was employed, as a graphical pre and post-processing tool, to simulate saturated three-dimensional groundwater flow using the USGS numerical code MODFLOW-2000 (Harbaugh et al. 2000). Overall, the flow model domain has an area of 1,600 m^2 (Fig. 2). In the horizontal plane the model domain was discretized by a regularly spaced grid of 0.5 × 0.5 m. Vertically, between 4.3 and −1.7 m a.s.l., the model domain was discretized into six layers each of 1 m thickness.

Different methods for permeability field representation were considered and compared as summarized in Table 2. The summary of the statistical analysis of the nine simulations are reported in Table 5. In the first five scenarios the sole hydrogeological dataset is employed; while, in the last four resistivity derived permeability were taken into consideration. Details of the analyzed scenarios are as follows:

Scenario 1: at the top three layers an average permeability value, derived from laboratory tests on samples collected from P1 and P2 at 2 m a.s.l., was assigned; at the bottom three layers an average permeability value derived from laboratory tests on samples collected at 1 m a.s.l., was assigned.

Scenario 2: a single permeability value from depth integrated slug test on C3, was input for the whole domain. Since an horizontal stratification was evident from core samples, a vertical anisotropy (the ratio between horizontal and vertical hydraulic conductivity) equal to 5 was assumed, as this is a typical value for sedimentary formations (Todd 1980).

Scenario 3: the permeability field was interpolated with Ordinary Kriging (Swan and Sandilands 1995) from depth integrated slug tests conducted on five piezometers and the vertical anisotropy was fixed to 5.

Scenario 4: the permeability field was interpolated with Ordinary Kriging from depth integrated slug tests conducted on all the 13 piezometers and the vertical anisotropy was also fixed to 5.

Scenario 5: the permeability field derived from multilevel slug tests carried out on all the 13 piezometers was assigned; in particular, conductivity values for the top 2 layers refer to slug tests undertaken between 2.4 and 1.9 m a.s.l., for the mid 2 layers reference was made to slug tests conducted between 1.4 and 0.9 m a.s.l. while for the

Table 2 Different scenarios implemented; note that for each ERT profile the number of data point collected is approximately 1,000

Scenarios	Description	Piezometers	Depth (m a.s.l.)	ERT profile	Total # of field data
Sc_1	Auger	P1, P2	2 and 1	NONE	4
Sc_2	Slug test	C3		NONE	1
Sc_3	Slug tests	C1, C3, C5, A3, E3		NONE	5
Sc_4	Slug tests	ALL 13		NONE	13
Sc_5	Slug tests	ALL 13	2.4/1.9, 1.4/0.9, 0.4/−0.1	NONE	39
Sc_6	Auger + ERT	P1, P2	2 and 1	ALL 4	4 + 4
Sc_7	Slug tests + ERT	C1, C3, C5, A3, E3		ALL 4	5 + 4
Sc_8	Slug tests + ERT	ALL 13		ALL 4	13 + 4
Sc_9	Slug tests + ERT	ALL 13	2.4/1.9, 1.4/0.9, 0.4/−0.1	ALL 4	39 + 4

bottom 2 layers to those carried out between 0.4 and 0.1 m a.s.l.

Scenario 6: hydraulic conductivity values assigned in Scenario 1 were plotted against the corresponding true electrical resistivity values (Fig. 4) to derive the site-specific coefficient for the log–log linear correlation found for the LA.R.A. test site (see "Hydraulic-electrical conductivity relationship"). The resulting equation was used to transform resistivity values in hydraulic conductivity values (more than 600 data per layer). The latest were assigned to the model domain using Ordinary Kriging interpolation method.

Scenario Nos. 7, 8 and 9: the permeability distribution was obtained by adding the resistivity derived permeabilities to the distributions reported in scenarios Nos. 3, 4 and 5.

A fully transient 3D flow model was implemented and calibrated versus continuous heads monitoring in 4 observation wells and versus groundwater level data from 13 observation wells, recorded in three piezometric campaigns. The overall simulation time of 52 days (from 17 June 2007 to 8 August 2007) was subdivided into 40 different stress periods to capture and accurately simulate levels' fluctuation in the canals. MODFLOW-2000's Time-Variant Specified-Head Package (Harbaugh et al. 2000) was used to represent the northern and southern boundaries and their influence on local flow pattern; this package allows the specified heads to be linearly interpolated in time between the beginning and the end of each stress period, such that the specified head for a grid cell may change at each time step of a given stress period. The northern and southern boundaries are not hydrogeological boundaries but they were set at the location of piezometers P1 and P2 and groundwater level records were used as input for the Time-Variant Specified-Head Package. No flow was assumed along the eastern and western sides, as ERT results indicated the closure of the paleo-channel towards these model boundaries (Fig. 2). Recharge and evapotranspiration during the simulated period were neglected across the model domain (see "Hydrogeological surveys").

The automated inverse model PEST (Doherty 2002) was used to quantify parameter's sensitivity, that is, to quantify the uniqueness and goodness of the hydraulic conductivity field reconstruction. The composite sensitivity is defined as the composite derivative of the calculated results at all observation points with respect to the specified parameter (Doherty 2002). Using the additive approach, the permeability field in all the scenarios can be lumped in a single adjustable parameter, thus the comparison between different sensitivity analyses becomes easier than using the classical zonation approach, where the domain is subdivided into zones of constant k (Hill 1998). This additive approach permits the ordinary used interpolation methods, like kriging or distance weighting, to be utilized to create smooth variations in values throughout the model domain (Harbaugh et al. 2000).

Results

Hydraulic-electrical conductivity relationship

The inverted 2D resistivity models well match each other and their interpretation in terms of lithology was consistent with the site stratigraphy. All resistivity data have been processed to produce a pseudo-3D volume of the test site (Fig. 3). Many examples reported in the literature indicate that pseudo-3D inversion is a reasonable approach for practical application (Dahlin and Loke 1997; Bernstone et al. 1997; Dahlin et al. 2007). Anywhere the lateral effects are relatively small, 2D inversion results can be confidently performed; moreover, in order to increase the reliability of this assumption, Wenner array can be preferred because of its low off-line sensitivity (Dahlin and Loke 1997; Dahlin et al. 2007; Loke 2004).

Once we have good 2D results we can put them together; of course 2D section merging makes sense only when non-severe changes occur between profiles.

When these assumptions are not matched, e.g., in more strongly variable environments, 3D data acquisition and the corresponding 3D inversion must be used in order to provide accurate reconstruction of 3D electric structures. In these cases, if we attempt to follow the approach presented in this paper without a truly three-dimensional acquisition and processing, a site-specific relation between the electrical and

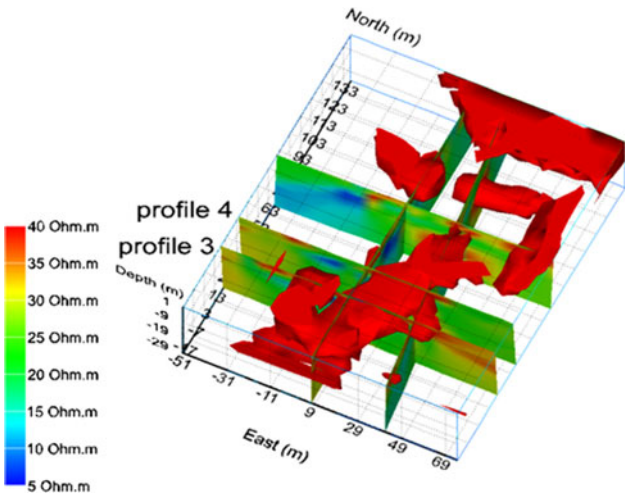

Fig. 3 Pseudo-3D representation of the inverted 2D resistivity profiles; *red* colored volumes represent sandy bodies where the hydrogeological test site has been established

hydraulic properties could be hard to deduce and, even worse, wrongly inferred hydraulic conductivities might be located in mistaken places.

The disadvantage of a real 3D survey is that this kind of acquisition is much more demanding and expensive.

The pseudo-3D reconstruction (Fig. 3) shows a resistivity sequence formed by sandy bodies characterized by some lateral heterogeneities attributed to the presence of silty-clay materials. The elongated resistivity volume (shown in red) with resistivity values greater than 40 Ω m was interpreted to be sand belonging to the paleo-channel. This elongated anomaly was selected to set-up the hydrogeological test site. The correspondence between inverted resistivity values and lithology was done through the drilling of 13 shallow boreholes (Fig. 2) and two auger boreholes (Fig. 4); this resistivity-lithology calibration confirmed the preliminary assumptions and is reported in Table 3.

The hydraulic conductivity (k) data derived from hydrogeological characterization (slug tests and Darcy laboratory tests) have been compared with electrical resistivity ($1/\sigma$) inverted data. As a result a simple log–log linear relationship between these two parameters was found (Fig. 5).

Hydrogeological surveys

Grain size distribution in the 2 auger boreholes, shows that P1 is characterized by sandy sediments and P2 by sandy loam sediments (Fig. 4), this is in good agreement with Darcy laboratory tests (Table 4).

Results from permeability tests plotted in Fig. 5, show that measured values of hydraulic conductivity vary over nearly four orders of magnitude, from $9.3e^{-4}$ to $1.5e^{-7}$ m/s

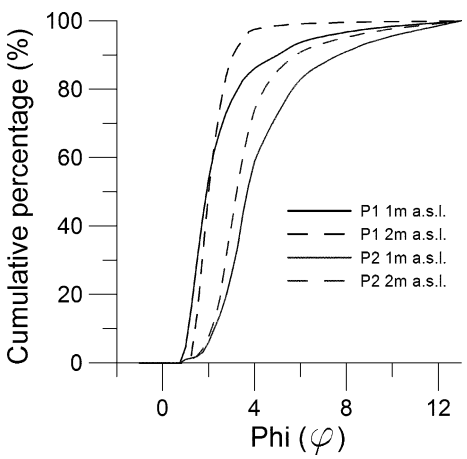

Fig. 4 Cumulative percentage plot of sediments collected in P1 and P2, abscissa is expressed in Phi diameter, computed by taking the negative log of the diameter in millimeters

Table 3 Correspondence between resistivity and lithology through L.A.R.A

Site obtained using 13 shallow boreholes (Fig. 2)

Resistivity (Ω m)	Lithology
<15	Clay
15–25	Silty-clay
25–35	Loam
>35	Sandy silt

exactly (Table 4). The estimated k values, by means of the automatic curve matching of AQTESOLV software, resulted in low values of the weighted residuals: the mean, the sum of squares and the standard deviation of all data been, respectively, 0.004 m, $9.3e^{-5}$ m^2 and 0.007 m.

The geometric mean hydraulic conductivity is $2e^{-5}$ m/s. Zones of relatively low hydraulic conductivity exist directly below zones of high hydraulic conductivity, interpreted as the bottom of unconfined aquifer. The 20% of tested intervals yielded hydraulic conductivities greater than $5e^{-5}$ m/s (Table 4). With respect to hydrostratigraphic characterization, these intervals are considered as high-permeability zones within the aquifer. Unfortunately, without other additional information these zones cannot be implemented in a flow model with sufficient resolution; this means, that without any geophysical survey an average constant hydraulic conductivity should be applied for modeling purposes; otherwise an interpolation can be attempted but without geostatistical meaning.

Plotting hydraulic conductivity data versus electrical resistivity data a positive linear correlation was found, independently from the methodology applied to acquire the permeability data (Fig. 5). Weighing depth specific values of permeability against resistivity (Scenario 6, Table 2) resulted in a very good fit with a correlation coefficient R^2 of 0.87, most probably as a consequence of the small number of measurements. Using depth integrated hydraulic conductivity data from Scenario 7 and Scenario 8 a weak correlation was found with R^2 close to 0.5 and 0.7, respectively. Finally in Scenario 9, using depth specific values of permeability, a 0.8 R^2 confirmed the good correlation between hydraulic conductivity and electrical resistivity at the test site. Thus, increasing the number of data constraining the empirical correlation leaded to a better fit. Since the piezometers where screened also in the low permeability sediments below the paleo-channel body, the permeability determined in the lower part of the screens was considered representative of the low permeability sediments surrounding the paleo-channel.

The second step in hydrogeologic site investigation regarded the continuous monitoring of hydraulic heads, which leaded to identify groundwater drainage directions. During the monitoring period, groundwater temperature and electrical conductivity remained nearly constant;

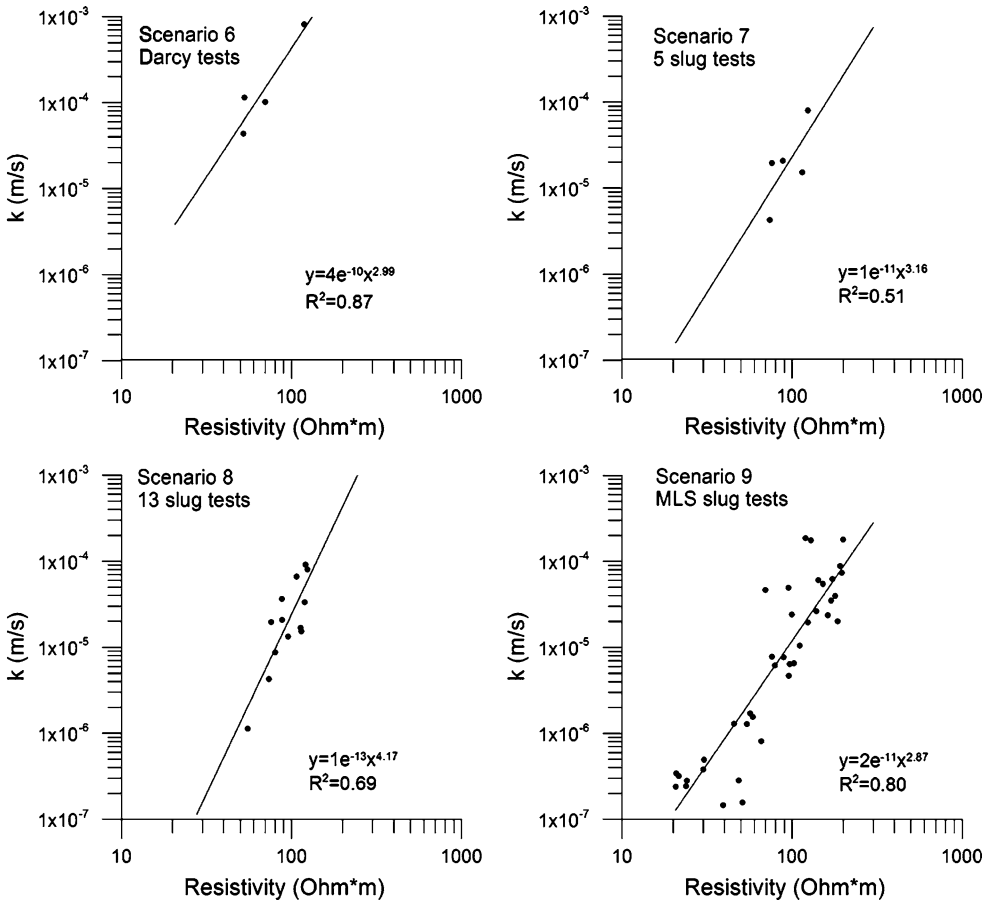

Fig. 5 Log–log plot of resistivity, hydraulic conductivity and fitted curves, for scenarios 6, 7, 8 and 9

Table 4 Hydraulic conductivity distribution in the field site

Piezometers	Description	*k* (m/s) at 2 m a.s.l.	*k* (m/s) at 1 m a.s.l.	*k* (m/s) at 0 m a.s.l.	*k* (m/s) whole depth
P1	Grain size analysis	9.29E−04	3.91E−04	Not measured	6.60E−04
P1	Darcy lab. test	8.12E−04	1.14E−04	Not measured	4.63E−04
P2	Grain size analysis	1.30E−04	1.00E−05	Not measured	7.00E−05
P2	Darcy lab. test	1.02E−04	4.35E−05	Not measured	7.28E−05
A3	Slug test	2.44E−07	7.72E−06	5.46E−05	2.09E−05
B2	Slug test	3.20E−07	3.51E−05	4.69E−06	1.34E−05
B3	Slug test	2.84E−07	3.97E−05	1.06E−05	1.69E−05
B4	Slug test	2.40E−07	1.96E−05	6.43E−06	8.76E−06
C1	Slug test	1.47E−07	6.53E−06	6.17E−06	4.28E−06
C2	Slug test	2.81E−07	2.63E−05	7.38E−05	3.35E−05
C3	Slug test	3.81E−07	6.04E−05	1.80E−04	8.03E−05
C4	Slug test	4.93E−07	1.75E−04	2.36E−05	6.64E−05
C5	Slug test	4.93E−05	7.81E−06	1.71E−06	1.96E−05
D2	Slug test	8.13E−07	1.29E−06	1.29E−06	1.13E−06
D3	Slug test	3.43E−07	6.27E−05	4.67E−05	3.66E−05
D4	Slug test	1.57E−07	8.89E−05	1.86E−04	9.17E−05
E3	Slug test	1.56E−06	2.01E−05	2.43E−05	1.53E−05
Average *k* (m/s)		1.19E−04	6.53E−05	4.77E−05	1.43E−04

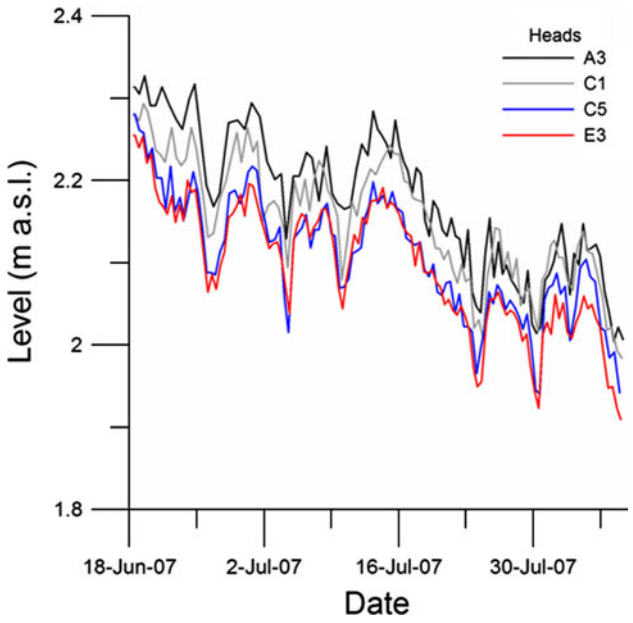

Fig. 6 Record of observed heads in four different observation wells

instead, water table decreased by 0.35 m in the four observation wells. The piezometric drawdown over the 52 days observation period is likely to be due to canals' level lowering over summer season (Fig. 6). Daily head peaks, in the decreasing trend of the water table, are almost certainly due to irrigation activities in the nearby cultivated fields.

Head difference between observation wells remained constant during the monitored period which confirms the general groundwater flow direction from SW (piezometer A3 in Fig. 2) to NE (piezometer E3 in Fig. 2). The thermo-pluviometric station of the F.lli Navarra Foundation for Agriculture, located approximately 100 m south of the model domain, did not register any rainfall event in the considered period of monitoring.

Discussion

Model results

Since the model boundary conditions implemented are simple (only fixed heads and no-flow boundaries) the water table contours are not complex, with an almost flat head gradient in the high-permeability zones and steep one in low permeability zones (Fig. 7). Accordingly, a bending of piezometric contours occurs at the interface between high and low permeability zones.

The final model (Scenario 9), implemented with all available field data, shows an absolute residual mean error of 0.022 m and a normalized root mean square (RMS) of 6.71% (Fig. 7). Model results replicate the transient water table drawdown related to canals' level fluctuation (Fig. 6) of about 0.35 m during the simulated period. Also, the contour map of calculated heads shows a simple flow pattern from south to north with variable hydraulic gradient and convergent and divergent flow directions indicating local heterogeneities within the model domain.

The fit between calculated and observed heads for the nine simulated scenarios, was compared using classical statistic operators to quantify the contribution of permeability fields derived from the ERT data (Table 5). Plotting the standard error of the estimate and the RMS (Fig. 8), it is evident that the introduction of the ERT derived permeability field has substantially improved the fit between observed and calculated heads.

From Fig. 8 it is also clear that the use of depth specific hydraulic conductivity data (Scenario 5) did not improve significantly model results with respect to the ones obtained using depth integrated hydraulic conductivity data (Scenario 4). This arises from the strong influence of the sharp physical boundaries which cause a sudden change in permeability (between paleo-channel and silty-clay sediments). The

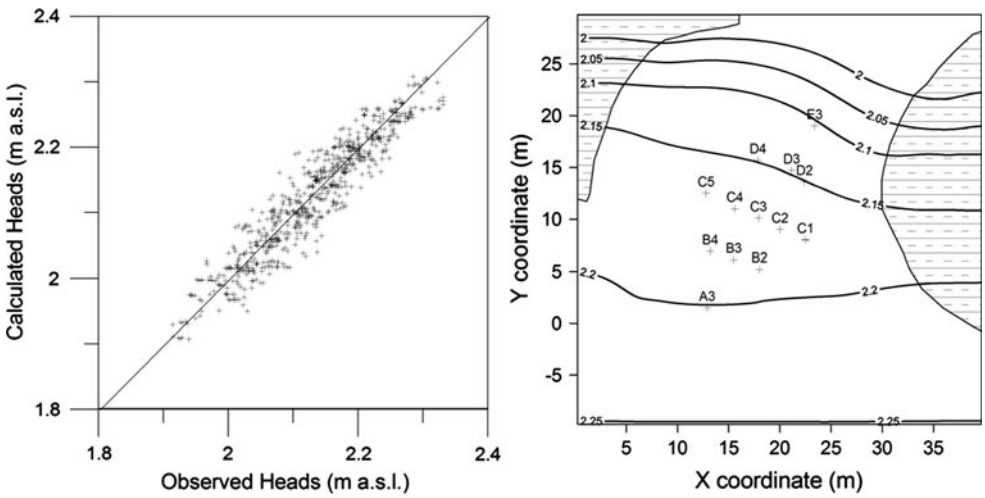

Fig. 7 Scatter diagram comparing observed and computed heads in all observation wells (*left*), calculated heads map in layer 4 at day 02 July 2007, crosses are piezometers location and *dashed areas* are low permeability sediments (*right*)

Table 5 Calibration statistics report for the different scenarios implemented

Scenarios	Residual mean (m)	Abs. residual mean (m)	Standard error of estimate (m)	Root mean squared (m)	Normalized RMS (%)	Correlation coefficient (R^2)
Sc_1	−0.098	0.098	2.5e−3	0.106	25.449	0.843
Sc_2	−0.095	0.095	2.3e−3	0.105	25.130	0.811
Sc_3	0.058	0.067	2.0e−3	0.081	19.297	0.827
Sc_4	−0.096	0.097	2.1e−3	0.111	26.659	0.839
Sc_5	0.090	0.091	2.0e−3	0.103	24.729	0.871
Sc_6	−0.029	0.034	1.4e−3	0.042	10.091	0.941
Sc_7	0.002	0.027	1.1e−3	0.034	8.098	0.926
Sc_8	−0.006	0.024	9.6e−4	0.030	7.296	0.944
Sc_9	−0.001	0.022	8.9e−4	0.026	6.710	0.964

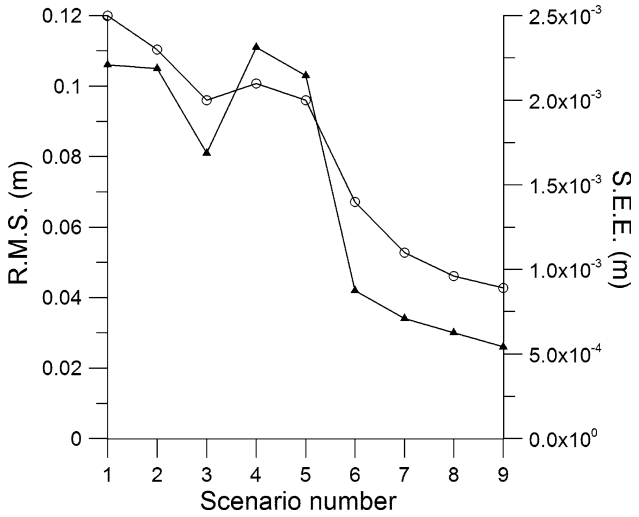

Fig. 8 Comparison of model fit (*circles* are ARM and *triangles* are Norm. RMS) for different permeability fields used as model input in different scenarios

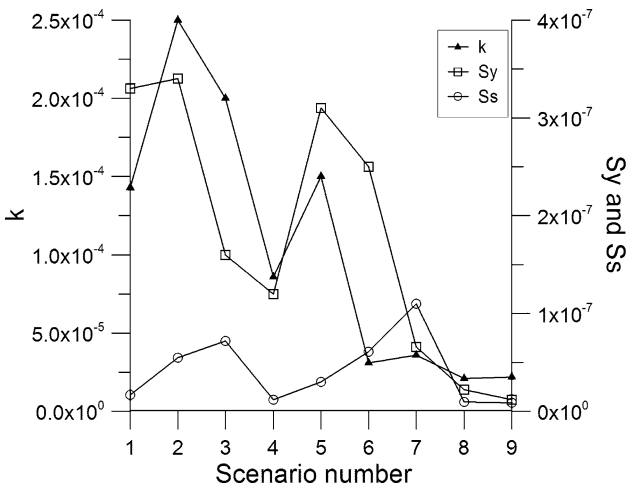

Fig. 9 Composite sensitivities of k, S_y and S_s for the different simulated scenarios

detection of these sharp boundaries cannot be resolved with the distribution of observation wells at the L.A.R.A. test site which were all drilled inside the paleo-channel (Fig. 2); instead, employing the ERT derived permeability information, a good approximation of these physical boundaries can be gained and consequently model results better agree with observed heads.

Sensitivity analysis

The sensitivity of the computed heads due to a parameter perturbation was tested for the model parameters listed in Table 1, excluding the average hydraulic gradient which was considered known.

As expected, the most sensitive parameter is the hydraulic conductivity in all the simulated scenarios, while S_y and S_s are quite insensitive parameters (Fig. 9), lying a couple of order of magnitude below k. For this reason a single value of S_y and S_s was used in all simulation. S_s sensitivity is also not influenced by the introduction of the ERT permeability derived values in the modeling process (Fig. 9). Moreover, a decrease in k and S_y sensitivities is observed by increasing the number of inputs which further constrained the numerical model (Fig. 9). Sensitivity analysis results highlight that the minimum number of measurements to safely characterize the selected aquifer portion is met in scenario 7 (total number of field data equal to 9 as shown in Table 2), where ERT profiles and field site slug tests are added to constrain the model simulation. The following scenarios even adding more informations, up to a total number of field data equal to 43, do not increase considerably the goodness of the model results.

Conclusions

To summarize and conclude, in this work groundwater flow simulation was carried out to assess the role of the resistivity

derived hydraulic conductivity distribution in the hydrogeological characterization of the L.A.R.A. alluvial test site. The resistivity data were useful also in the preliminary geolithological characterization of the test site, which leads to the correct positioning of the monitoring wells.

Wells allowed local measurements of hydraulic properties to be conducted. Consequently, a log–log linear relationship matching electrical and hydraulic conductivity has been obtained. By using this relationship the spatial distribution of the hydraulic conductivity values has been reconstructed and was incorporated in the groundwater flow model.

Results from numerical scenarios representing different approach to describe the in situ permeability field distribution, showed a substantial improvement of numerical model fit when the ERT derived permeability values are directly incorporated as model constraints. Thus, groundwater modeling confirmed that the combined geophysical and hydrogeological approach, employed in this work, is suitable and cost-effective. This technique can be applied to improve the monitoring of pollutants fate and transport along paleochannels, helping to better delineate physical boundaries and permeability variations, if groundwater electrical conductivity at the field site remains approximately constant.

Acknowledgments The work presented in this paper was financially supported by the ENVIREN-L.A.R.A. project, under PRRIITT-3.4A fund. Authors are grateful to Fondazione Fratelli Navarra (Ferrara, Italy) for its support and especially to Dr. Pier Carlo Scaramagli, Prof. Alessandro Bruni, Dr. Marco Rivaroli and Mr. Andrea Biondi. Prof. Torquato Nanni, Prof. Giovanni Santarato are gratefully acknowledged for their precious comments and suggestions. Authors thanks are also due to Dr. Stefano Palpacelli, Dr. Umberto Tessari and Dr. Enzo Salemi for field and laboratory assistance.

References

Ahamed S, de Marsily G, Talbot A (1987) Combined use of hydraulic and electrical properties on an aquifer in a geostatistical estimation of transmissivity. Ground Water 26(1):78–86

Amorosi A, Colalongo ML, Fusco F, Pasini G, Fiorini F (1999) Glacio-eustatic control of continental-shallow marine cyclicity from Late Quaternary deposits of the south-eastern Po Plain (Northern Italy). Quat Res 52:1–13

Amorosi A, Centineo MC, Colalongo ML, Pasini G, Sarti G, Vaiani SC (2003) Facies architecture and latest Pleistocene–Holocene depositional history of the Po Delta (Comacchio area), Italy. J Geol 111:39–56

Barlebo HC, Hill MC, Rosberg D (2004) Investigating the macrodispersion experiment (MADE) site in Columbus, Mississippi, using a three-dimensional inverse flow and transport model. Water Resour Res. doi:10.1029/2002WR001935

Bernstone C, Dahlin T, Jonsson P (1997) 3D visualization of a resistivity data set—an example from a sludge disposal site: SAGEEP'97, Reno, Nevada, pp 917–925

Bouwer H, Rice RC (1976) A slug test for determining hydraulic conductivity of unconfined aquifers with completely or partially penetrating wells. Water Resour Res 12(3):423–428

Bowling JC, Rodriguez AB, Harry DL, Zheng C (2005) Delineating alluvial aquifer heterogeneity using resistivity and GPR data. Ground Water 43(6):890–903

Bowling JC, Zheng C, Rodriguez AB, Harry DL (2006) Geophysical constraints on contaminant transport modeling in a heterogeneous fluvial aquifer. J Cont Hydrol 85:72–88

Butler JJ Jr, McElwee CD, Liu W (1996) Improving the quality of parameter estimates obtained from slug tests. Ground Water 34(3):480–490

Cardenas MB, Zlotnik VA (2003) Three-dimensional model of modern channel bend deposits. Water Resour Res 39(6):1141

Cassiani G, Medina MAJ (1997) Incorporating auxiliary geophysical data into groundwater flow parameter estimation. Ground Water 35(1):79–92

Dahlin T, Loke, MH (1997) Quasi-3D resistivity imaging-mapping of three dimensional structures using two dimensional DC resistivity techniques. In: Proceedings of 3rd meeting of the Environmental and Engineering Geophysical Society, pp 143–146

Dahlin T, Wisén R, Zhang D (2007) 3D effects on 2D resistivity imaging—modelling and field surveying results. In: Proceedings of 13th European meeting of Environmental and Engineering Geophysics

Dam D, Christensen S (2003) Including geophysical data in ground water model inverse calibration. Ground Water 41(2):178–189

Dinelli G, Accinelli C, Vicari A, Catizone P (2000) Comparison of the persistence of Atrazine and Metolachlor under field and laboratory conditions. J Agric Food Chem 48:3037–3043

Doherty J (2002) PEST—model-independent parameter estimation. User's manual, 5th edn. Watermark Computing, Brisbane, Australia

Duffield GM (2002) AQTESOLV for Windows User's Guide. HydroSOLVE, Inc., Reston, VA

Harbaugh AW, Banta ER, Hill MC, McDonald MG (2000) MODFLOW-2000, The U.S. G. S. modular ground-water model User guide to modularization concepts and the ground-water flow process, U. S. G. S. Open-file report 00-92

Hazen A (1911) Discussion: dams on sand foundations. Trans Am Soc Civil Eng 73:199

Heigold PC, Gilkeson RH, Cartwright K, Reed PC (1979) Aquifer transmissivity from surficial electrical methods. Ground Water 17:338–345

Hess KM, Wolf SH, Celia MA (1992) Large-scale natural gradient tracer test in sand and gravel, Cape Cod, Massachusetts. Hydraulic conductivity variability and calculated macrodispersivities. Water Resour Res 28:2011–2027

Hill MC (1998) Methods and guidelines for effective model calibration. U.S. Geological Survey, Water-Resources Investigations Report 98-4005

Hubbard SS, Rubin Y (2000) Hydrogeological parameter estimation using geophysical data: a review of selected techniques. J Cont Hydrol 45:3–34

Hyder Z, Butler JJ Jr (1995) Slug tests in unconfined formations: an assessment of the Bouwer and Rice technique. Ground Water 33(1):16–22

Kelly WE (1977) Geoelectric sounding for estimation of aquifer hydraulic conductivity. Ground Water 15(6):420–425

Kosinski WK, Kelly WE (1981) Geoelectric soundings for predicting aquifer properties. Ground Water 19:163–171

Linde N, Binley A, Tryggvason A, Pedersen L, Revil A (2006) Improved hydrogeophysical characterization using joint inversion of cross-hole electrical resistance and ground-penetrating radar traveltime data. Water Resour Res 42:W12404. doi:10.1029/2006WR005131

Loke MH (2001) Rapid 2D and 3D Resistivity and IP inversion using the least squares method—RES2DINV Ver 3.4 Manual. Available via DIALOG. http://www.geoelectrical.com

Loke MH (2004) Tutorial: 2D and 3D electrical imaging surveys. Available on http://www.geoelectrical.com

Mastrocicco M, Colombani N, Palpacelli S (2008) Fertilizers mobilization in alluvial aquifer: laboratory experiments. Environ Geol. doi:10.1007/s00254-008-1232-1

Mazac O, Cislerova M, Vogel T (1985) A hydrogeophysical model for relations between electrical and hydraulic properties of aquifers. J Hydrol 79:1–19

Ponzini G, Ostroman A, Molinari M (1983) Empirical relation between electrical transverse resistance and hydraulic transmissivity. Geoexploration 22:1–15

Purvance DT, Andricevic R (2000) On the electrical-hydraulic conductivity correlation in aquifers. Water Resour Res 36:2905–2913

Rehfeldt KR, Boggs JM, Gelhar LW (1992) Field study of dispersion in a heterogeneous aquifer: geostatistical analysis of hydraulic conductivity. Water Resour Res 28:3309–3324

Rovey CW, Niemann WL (2001) Wellskins and slug tests: where's the bias? J Hydrol 243:120–132

Slater L (2007) Near surface electrical characterization of hydraulic conductivity: from petrophysical properties to aquifer geometries—a review. Surv Geophys. doi:10.1007/s10712-007-9022-y

Swan ARH, Sandilands M (1995) Introduction to geological data analysis. Blackwell Science Ltd., Oxford

Todd DK (1980) Groundwater hydrology. Wiley, New York

Urish DW (1981) Electrical resistivity-hydraulic conductivity relationships in glacial outwash aquifers. Water Resour Res 17(5):1401–1408

Zlotnik V (1994) Interpretation of slug and packer tests in anisotropic aquifers. Ground Water 32(5):761–766